SCIENTIFIC COMMITTEE
NINETEENTH REGULAR SESSION

Koror, Palau
16 – 24 August 2023

Target Strength Measurements of *Ex-Situ* Yellowfin Tuna (*Thunnus Albacares*) and Frequency-Response Discrimination for Tropical Tuna Species

WCPFC-SC19-2023/EB-IP-19

Bea Sobradillo[1], Guillermo Boyra[2], Jon Uranga[2] and Gala Moreno[3]

[1] AZTI, Marine Research, Basque Research and Technology Alliance (BRTA), Txatxarramendi Ugartea Z/G, Sukarrieta, Spain
[2] Azti, AZTI, Marine Research, Basque Research and Technology Alliance (BRTA), Muelle de la Herrera, Zona Portuaria s/n – 20110 Pasaia, Gipuzkoa, Spain
[3] International Seafood Sustainability Foundation (ISSF), 1440 G Street NW, Washington, DC 20005, USA

TS MEASUREMENTS OF *EX-SITU* YELLOWFIN TUNA *(THUNNUS ALBACARES)* AND FREQUENCY-RESPONSE DISCRIMINATION FOR TROPICAL TUNA SPECIES

Bea Sobradillo [1], Guillermo Boyra [2], Jon Uranga [2] and Gala Moreno [3]

[1]*AZTI, Marine Research, Basque Research and Technology Alliance (BRTA), Txatxarramendi Ugartea Z/G, Sukarrieta, Spain*

[2]*Azti, AZTI, Marine Research, Basque Research and Technology Alliance (BRTA), Muelle de la Herrera, Zona Portuaria s/n – 20110 Pasaia, Gipuzkoa, Spain*

[3]*International Seafood Sustainability Foundation (ISSF), 1440 G Street NW, Washington, DC 20005, USA*

SUMMARY

Tuna fisheries support one of the world's most valuable markets, with over 50% of the catch coming from drifting fish aggregating devices (DFADs). To locate and quantify tuna on DFADs, fishermen mostly use acoustic technologies, which significantly reduce the nominal fishing effort, especially in tropical purse seine fisheries. However, to date, discrimination between species using purely acoustic methods has not been refined due to a lack of information on the acoustic response of each species at different frequencies. Three tuna species can be found simultaneously at DFADs: skipjack or SKJ (*Katsuwanus pelamis*), bigeye or BET (*Thunnus obesus*), and yellowfin or YFT (*Thunnus albacares*), of which only the acoustic frequency responses of SKJ and BET have been published. In this study, we present the frequency response obtained from ex situ measurements of YFT recorded at 38, 70, 120 and 200 kHz. Records based on two data sets were used to describe the relationship between acoustic signal or target strength (TS; dB re 1m2) and fish length across frequencies. The results described a flat response across frequencies, with b20 (standard deviation) values of -71.5 (11), -72.3 (11), -71.6 (10), and -72.3 (11) dB at 38, 70, 120, and 200 kHz, respectively. These results, combined with previously published increasing (SKJ) and decreasing (BET) responses, were used to develop a discrimination algorithm for these 3 species. The algorithm was tested using acoustic data and catches from commercial campaigns aboard a tuna vessel.

INTRODUCTION

More than half of the purse seine landings targeting tropical tunas come from fishing with Fish Aggregating Devices (DFADs). These have sophisticated acoustic sensors on board (vertical and side-looking echosounders, as well as long-range multibeam sonar) in addition to satellite buoys equipped with low-cost acoustic echosounders, to allow fishermen to decide on which FAD to visit. The use of acoustic devices before setting the nets improves the selectivity of the catch (Lopez *et al.*, 2014; Moreno *et al.*, 2016). However, few studies have been published on the acoustic characteristics of the species present at FADs (Bertrand, 1999; Lu *et al.*, 2011; Boyra *et al.*, 2018, 2019), and most of the recorded data are currently underutilized, hampering their potential to provide information on the location, composition and abundance of species from a distance. There are mainly three tropical tuna species that can be aggregated simultaneously in FADs (Fonteneau *et al.*, 2013): skipjack or SKJ (*Katsuwanus pelamis*), bigeye or BET (*Thunnus obesus*), and yellowfin or YFT (*Thunnus albacares*). Since 2014, AZTI, in collaboration with ISSF, has been conducting a series of studies to improve the discrimination between species and the determination of average size of tuna using both echosounder data and sonar from the tuna vessels themselves. The first step in developing acoustic methods for species discrimination is to determine the sound scattering properties of each species separately, which are mainly defined by the backscattering cross-section (σ_{bs}; m^2) and its logarithmic form, the target strength (TS; dB re 1 m^2] (MacLennan *et al.*, 2002). So far, during the four surveys conducted (three in the Atlantic and one in the Pacific), it has been possible to determine the acoustic characteristics of two of the three main species fished in the DFADs: skipjack (Boyra et al., 2018) and bigeye tuna (Boyra et al., 2019), and to take the first steps towards the acoustic discrimination of tropical tunas (Moreno *et al.*, 2019). The main objective of the present work is to determine the acoustic properties, mainly the TS(*f*) and TS(*L*) relationships, of small-sized yellowfin tunas in captivity and combine them with the previously published results of SKJ and BET to develop an acoustic discrimination algorithm for tropical tunas (Moreno *et al.*, 2019).

MATERIALS AND METHODS

The experiments were conducted at the IATTC Achotines Laboratory, located in Achotines Bay, Panama **(Figure 1)**. The first measurements were made in July 2016 (days 27, 28 and 29), and the final measurements were between May 24 and June 22 of year 2022. The experiments were conducted in an *offshore* cage with a diameter of 25 meters and a depth of just under 20 meters. The experiments consisted of capturing yellowfin tuna, transporting them alive to the cage and then recording measurements with scientific acoustic equipment to study the acoustic

characteristics of this species. Once the acoustic measurements were completed, the cage was dismantled and all specimens were removed for biological sampling (length, width, height and weight of each fish) and X-rays to study the swimbladder morphology (**Figure 2, Table 1**).

Acoustic sampling. A Simrad EK60 scientific echosounder with three split-beam transducers at 38, 120 and 200 kHz was used in 2016, and an EK80 with four split-beam transducers (38, 70, 120 and 200 kHz) was used for the 2022 measurements. All transducers had a 7-degree opening beam and were vertically oriented downwards with an emitted pulse duration of 0.512 ms in CW mode. The maximum nearfield effect was determined as the sum of the emitted and backscattered fields, from the transducer and the fish body, respectively. With this in mind, and being rather conservative, the minimum depth at which data were considered reliable in this study was set at 10 m.

The transducers were mounted on a steel plate, with a flotation system and a weight to keep it stable below the surface line. The electronics were installed on a vessel with a battery system for power supply and awnings to protect the computers from sunlight and rain. Calibration was performed prior to data collection, using a 38.1 mm tungsten sphere at a depth of 24.5 m with the settings specified in **Table 2** and following the standard target method (Demer *et al.*, 2015).

Data analysis. Acoustic recordings for TS estimation and TS-length relationship were made on live tuna in both the 2016 and 2022 sets **(Table 1, Figure 3)**. The study of the acoustic characteristics of live yellowfin tuna was conducted using target strength analysis (Simmonds and MacLennan, 2005), which consists of obtaining the echo of isolated yellowfin tuna targets in the 10-25 m depth range. The echosounder data were processed using commercial (Echoview; Hobart, Tasmania) and an open-source software (R, R Core Team, 2014). A single target detection algorithm (MacLennan and Menz, 1996; Soule *et al.*, 1996; Demer *et al.*, 1999) was used to discard unwanted echoes. The threshold for data analysis was set to -50 dB and other parameters were left as their default values (see **Table 3**). In addition, a target tracking analysis (Blackman, 1986) (see **Table 3**) was used to assign individual target detections to individual tracks and to obtain the fish orientation by comparing the displacements along the horizontal and vertical axes of the first and last echoes of each track.

The relationship between TS and fork length was modeled as a linear regression of the type:

$$TS = a \log_{10}(L) + b, \qquad \textbf{(Eq. 1)}$$

where the slope (*a*) was assumed to be 20 due to the small number of length samples available, insufficient to generate an experimental slope. The b20 (Simmonds and MacLennan, 2005) of yellowfin tuna was estimated for each frequency using the averaged length measurements. However, the central TS value per frequency was obtained as the mode of the TS histogram, after smoothing to a Gaussian density curve. This was done first to remove the effect of possible noise in the distribution, but also to remove the effect of the minimum threshold on the final central value. The mode of the distribution was then retained and used to obtain the TS(L) relationship.

Frequency response-based discrimination algorithm. To develop a discrimination algorithm for the three major tropical tuna species, two elements were used: (1) the individual frequency response patterns of the three species and (2) an optimization process to determine the interspecific classification limits of the algorithm. The frequency response patterns of each

individual species were obtained from the literature in the case of SKJ and BET (Boyra et al., 2018, 2019; Moreno et al., 2019) and from the present study for YFT, and were defined in terms of differences in mean volume backscattering strength (ΔMVBS) between frequency pairs **(Eq. 2)**. These individual responses were used to define generic classification rules dependent on undefined thresholds (to be defined in the optimization process):

$$Species = \begin{cases} SKJ,\ if & \begin{cases} MVBS_{38} - MVBS_{200} < A \\ MVBS_{38} - MVBS_{120} < B \end{cases} \\ BET,\ if & \begin{cases} MVBS_{38} - MVBS_{200} > C \\ MVBS_{38} - MVBS_{120} > D \end{cases} \\ YFT,\ if & \begin{cases} A < MVBS_{38} - MVBS_{200} < C \\ MVBS_{38} - MVBS_{120} < D \end{cases} \end{cases} \quad \textbf{(Eq. 2)}$$

To obtain the thresholds that optimized the algorithm performance, each condition was tested against multiple values to retain the thresholds that minimized the root mean square error (RMSE) between the predicted and observed species proportions. Once the optimal thresholds were defined, the RMSE metric was used to estimate the mask classification performance, both overall and by species.

RESULTS AND DISCUSSION

Biological sampling. A total of 6 specimens were used in the experiments (**Table 1**). Mean fork lengths of sets 1 and 2 were 52.7 cm and 51.4 cm, respectively. The swimbladder was elongated, from 2 to 3 times longer than it was wide and occupied approximately 21% (± 2.5) of the body length. It was tilted 25 ± 5 degrees from the horizontal axis of the body **(Figure 2)**.

TS distributions. The modes of the TS distributions observed from the measurements of live tuna in the cage were 2 to 4 dB higher in 2016 than in 2022. Set 1 had a central mode value of -36 dB at all frequencies and Set 2 had values of -38, -40, -40 and -34 dB at 38, 70, 120 and 200 kHz, respectively **(Figure 4)**.

TS versus depth. As recommended in previous studies the combined nearfields of the transducer and the swimbladder were considered when calculating the nearfield area in a cage (Rodríguez-Sánchez *et al.*, 2016; Puig-Pons *et al.*, 2022). The nearfied from the swimbladder covered distances from 0.8 m to 3.9 m at 38 and 200 kHz, respectively. Conversely, the nearfield from the transducer decreased with frequency, from 4.55 m at 38 kHz to 1.33 m at 200 kHz. The combined nearfields from the transducer and the fish were used to define a rather conservative depth threshold of 10 m. To test the variability of the data against depth, the distribution of TS values from both sets was compared at two depth layers: from the 10 to 15 m and from 15 to 20 m. The distributions across layers were not statistically different (p-value > 0.05), but the median values were about 5 dB lower at 15-20 m depth than at 10-15 m depth **(**Figure 5**)**. Physoclist species such as yellowfin tuna are capable of compensating for gas volume changes with depth (Blaxter and Batty, 1990), but as noted previously (Bertrand, 1999), volume changes resulting from rapid descent may not be compensated for immediately, but with some "lag", which would be consistent with the decrease observed in this study.

TS versus tilt angle. A total of 2000 tracks were used to extract the fish orientation in each track for the analysis of TS versus the apparent tilt angle of the fish. The distribution of angles fit a Loess smoothing, with maximum (smoothed) TS values of -37.5 ± 0.5 dB between -15 and -30 degrees (Figure 6), and the lowest of -43 ± 0.5 dB between 25 and 40 degrees. About 90% of the tracks were detected at 0 ± 15 degrees and only 5 tracks were tilted more than 75 degrees, either up or down. The contribution of the fish orientation to the variability of the TS values is a well-known issue (Dahl and Mathisen, 1983) that is mainly related to fish behaviour (McQuinn and Winger, 2003). Both analyses were consistent with previous studies (Bertrand, 1999; Lu *et al.*, 2011; Puig-Pons *et al.*, 2022) in that the highest backscatter was observed when tuna were descending with the swimbladder cross-section oriented perpendicular to the transducer beam **(**Figure 6**)**.

TS versus fish length. The smoothed Gaussian distributions gave central mode TS values at -40.7, -41.7, -39.4 and 38 dB at 38, 70, 120 and 200 kHz, respectively **(**Figure 7**)**. These values were used to fit the TS(*L*) model for each frequency, using the mean fork length of tuna at each set, yielding b_{20} values of -71.5(11), -72.3(11), -71.6(10) and -72.3(11) dB **(**Figure 8**)**. It is generally assumed that TS depends on fish size according to a specific relationship (**Eq. 1**), with parameters defined as a function of the growth rate of the resonant organs relative to the growth rate of the fish. When data are scarce, such as length in the present study, it has been widely assumed that the acoustic cross section is proportional to the horizontal section of the swimbladder, which is also proportional to the square of the fish length (Simmonds and MacLennan, 2005). This relationship implies that the *a* parameter in **Eq. 1** is 20, and the *b* parameter is then defined as $b_{20.}$ This assumption also allows the acoustic signal of the three tuna species of interest to be compared using the same parameters.

Frequency response of three tropical tuna. These results were combined with the previously published frequency response of BET and SKJ (Moreno *et al.*, 2019) (Figure 9), which showed that BET presented the highest b_{20} values of the three species at 38 and 120 kHz (-65.3 ± 8 and -65.6 ± 7 dB), with a decrease of almost 7 dB at 200 kHz. Conversely, the frequency response described by SKJ was low at 38 kHz (-76 dB) and increased by almost 6 dB at high frequencies. YFT described a flat frequency response, with variations of less than 1 dB across frequencies. In general, the BET response decreased with frequency, the SKJ response increased and the YFT response remained relatively flat across frequencies. The increasing or flat response is typical for swimbladdered fish (Fernandes *et al.*, 2006) as well as of other large physoclists (Pedersen *et al.*, 2004). On the other hand, SKJ does not have a swimbladder, which explains the increasing response pattern with frequency, as is the case in other non-swimbladdered species (Mosteiro *et al.*, 2004; Fernandes *et al.*, 2006; Korneliussen, 2010; Forland *et al.*, 2014).

Discrimination algorithm. Four different thresholds were obtained for each combination of frequencies used to resolve each of the three species. Thresholds A and B were used to discriminate SKJ, where a bin was assigned to SKJ if the echointegrated energy was 1.6 dB higher at 200 kHz than at 38 kHz, and 0.16 dB higher at 120 kHz than at 38 kHz. Thresholds C and D were used for BET classification, where bins with values 0.16 dB higher at 38 kHz than at 200 kHz and 0.016 dB higher at 120 kHz than at 200 kHz were assigned to BET. Finally, bins were assigned to YFT if the difference between 38 and 200 kHz was between -1.6 and 0.16, or between 120 and 200 was less than 0.016.

The result of the mask provided a deviation from the observed proportions of less than 10%, with the most accurately classified species being YFT. BET tended to be overestimated, while SKJ tended to be slightly underestimated **(**Figure 10**)**. The result of the mask per fishing operation provided RMSE values ranging from 1% to 47% **(**Figure 11**)**, with hauls 24, 26 and 27 of 2014 being the ones with the lowest error (less than 5%), and haul 4 of the same year providing the worst classification results, with the maximum error. Regarding the overall performance of the mask, the RMSE was 18.3%. The RMSE for BET and SKJ was close to 25%, while for YFT it was close to 11% **(**Figure 12**)**. These results are consistent with the first steps presented in *Moreno et al.* (2019), where echo integrated *Sv* values were used to describe the frequency response. As stated in the same study, some uncertainty will always remain as part of the stochasticity inherent in the target strength (Simmonds and MacLennan, 2005), but the monospecific acoustic records of yellowfin tuna collected in this study contributed significantly to reducing the uncertainty by increasing the acoustic dataset, as recommended therein. In addition, the availability of split-beam echosounders for TS estimation, as well as the reduced (or nonexistent) risk of detecting unresolved multiple targets (Soule *et al.*, 1996; Ona, E. and Barange, M., 1999), has greatly increased the potential of the knowledge gained, not only for species discrimination, but also for estimating the abundance of species present in the DFADs.

BIBLIOGRAPHY

Aglen, A. 1994. Sources of error in acoustic estimation of fish abundance. Marine Fish Behaviour in Capture and Abundance Estimation. Fishing.: 107–133. News Books.

Bard, F.-X., Bach, P., and Josse, E. 1998. Habitat, ecophysiologie des thons : quoi de neuf depuis 15 ans ?

Bertrand, A. 1999. In situacoustic target-strength measurement of bigeye (Thunnus obesus) and yellowfin tuna (Thunnus albacares) by coupling split-beam echosounder observations and sonic tracking. ICES Journal of Marine Science, 56: 51–60.

Bertrand, A. 2000. Tuna target-strength related to fish length and swimbladder volume. ICES Journal of Marine Science, 57: 1143–1146.

Blackman, S. S. 1986. Multiple-target tracking with radar applications. Dedham, MA, Artech House, Inc., 1986, 463 p.

Blaxter, J. H. S., and Batty, R. S. 1990. Swimbladder "behaviour" and target strength. Rapports et Proces-verbaux des Réunions du Conseil International pour l'Exploration de la Mer, 189: 233–244.

Boyra, G., Moreno, G., Sobradillo, B., Pérez-Arjona, I., Sancristobal, I., Demer, D. A., and Handling editor: Purnima Ratilal. 2018. Target strength of skipjack tuna (Katsuwanus pelamis) associated with fish aggregating devices (FADs). ICES Journal of Marine Science, 75: 1790–1802.

Boyra, G., Moreno, G., Orue, B., Sobradillo, B., and Sancristobal, I. 2019. In situ target strength of bigeye tuna (Thunnus obesus) associated with fish aggregating devices. ICES Journal of Marine Science: fsz131.

Dahl, P., and Mathisen, O. 1983. Measurement of fish target strength and associated directivity at high frequencies. The Journal of the Acoustical Society of America, 73: 1205–1211. Acoustical Society of America.

Dawson, J. J., Wiggins, D., Degan, D., Geiger, H., Hart, D., and Adams, B. 2000. Point-source violations: split-beam tracking of fish at close range. Aquat. Living Resour.

Demer, D. A., Soule, M. A., and Hewitt, R. P. 1999. A multiple-frequency method for potentially improving the accuracy and precision of in situ target strength measurements. The Journal of the Acoustical Society of America, 105: 2359–2376.

Demer, D. A., Berger, L., Bernasconi, M., and Eckhard, B. 2015. Calibration of acoustic instruments. ICES Cooperative Research Report, 326: 136.

Fernandes, P., Korneliussen, R., Lebourges-Dhaussy, A., Masse, J., Iglesias, M., Diner, N., Ona, E., *et al.* 2006. The SIMFAMI project: species identification methods from acoustic multifrequency information. Final Report to the EC, 2054.

Fonteneau, A., Chassot, E., and Bodin, N. 2013. Global spatio-temporal patterns in tropical tuna purse seine fisheries on drifting fish aggregating devices (DFADs): Taking a historical perspective to inform current challenges. Aquatic Living Resources, 26: 37–48.

Foote, K. G. 1985. Rather-high-frequency sound scattering by swimbladdered fish. The Journal of the Acoustical Society of America, 78: 688–700.

Foote K.G., Knudsen, H. P., Vestnes, G., MacLennan, D.N., and Simmonds, E. J. 1987. Calibraton of acoustic instruments for fish density estimation: a practical guide. ICES Cooperative Research Report. Copenhagen.

Forland, T. N., Hobæk, H., and Korneliussen, R. J. 2014. Scattering properties of Atlantic mackerel over a wide frequency range. ICES Journal of Marine Science, 71: 1904–1912.

Fréon, P., and Misund, O. A. 1999. Dynamics of pelagic fish distribution and behaviour: effects on fisheries and stock assessment. Fishing News Books, Oxford. 348 pp.

Furusawa, M. 1988. Prolate spheroidal models for predicting general trends of fish target strength. Journal of the Acoustic Society of Japan, 9.

Furusawa, M., Hamada, M., and Aoyama, C. 1999. Near Range Errors in Sound Scattering Measurements of Fish. Fisheries science, 65: 109–116.

Gastauer, S., Scoulding, B., and Parsons, M. 2017. Estimates of variability of goldband snapper target strength and biomass in three fishing regions within the Northern Demersal Scalefish Fishery (Western Australia). Fisheries Research, 193: 250–262.

Gerlotto, F., and Fréon, P. 1992. Some elements on vertical avoidance of fish schools to a vessel during acoustic surveys. Fisheries Research, 14: 251–259.

Godø, O. R., and Michalsen, K. 2000. Migratory behaviour of north-east Arctic cod, studied by use of data storage tags. Fisheries Research, 48: 127–140.

Hazen, E. L., and Horne, J. K. 2003. A method for evaluating the effects of biological factors on fish target strength. ICES Journal of Marine Science, 60: 555–562.

Knudsen, F. R., Fosseidengen, J. E., Oppedal, F., Karlsen, Ø., and Ona, E. 2004. Hydroacoustic monitoring of fish in sea cages: target strength (TS) measurements on Atlantic salmon (Salmo salar). Fisheries Research, 69: 205–209.

Komeyama, K., Kadota, M., Torisawa, S., Suzuki, K., Tsuda, Y., and Takagi, T. 2011. Measuring the swimming behaviour of a reared Pacific bluefin tuna in a submerged aquaculture net cage. Aquatic Living Resources, 24: 99–105.

Komeyama, K., Kadota, M., Torisawa, S., and Takagi, T. 2013. Three-dimensional trajectories of cultivated Pacific bluefin tuna Thunnus orientalis in an aquaculture net cage. Aquaculture Environment Interactions, 4: 81–90.

Korneliussen, R. J. 2010. The acoustic identification of Atlantic mackerel. ICES Journal of Marine Science: Journal du Conseil, 67: 1749–1758.

Lopez, J., Moreno, G., Sancristobal, I., and Murua, J. 2014. Evolution and current state of the technology of echo-sounder buoys used by Spanish tropical tuna purse seiners in the Atlantic, Indian and Pacific Oceans. Fisheries Research, 155: 127–137.

Lu, H.-J., Kang, M., Huang, H.-H., Lai, C.-C., and Wu, L.-J. 2011. Ex situ and in situ measurements of juvenile yellowfin tuna Thunnus albacares target strength. Fisheries Science, 77: 903–913.

MacLennan, D., Fernandes, P. G., and Dalen, J. 2002. A consistent approach to definitions and symbols in fisheries acoustics. ICES Journal of Marine Science, 59: 365–369.

MacLennan, D. N., and Menz, A. 1996. Interpretation of in situ target-strength data. ICES Journal of Marine Science: Journal du Conseil, 53: 233–236.

McQuinn, I. H., and Winger, P. D. 2003. Tilt angle and target strength: target tracking of Atlantic cod (Gadus morhua) during trawling. ICES Journal of Marine Science, 60: 575–583.

Midttun, L. 1984. Fish and other organisms as acoustic targets. *In* pp. 25–33.

Misund, O. A., Øvredal, J. T., and Hafsteinsson, M. T. 1996. Reactions of herring schools to the sound field of a survey vessel. Aquatic Living Resources, 9: 5–11.

Moreno, G., Dagorn, L., Capello, M., Lopez, J., Filmalter, J., Forget, F., Sancristobal, I., *et al.* 2016. Fish aggregating devices (FADs) as scientific platforms. Fisheries Research, 178: 122–129.

Moreno, G., Boyra, G., Sancristobal, I., Itano, D., and Restrepo, V. 2019. Towards acoustic discrimination of tropical tuna associated with Fish Aggregating Devices. PLOS ONE, 14: e0216353.

Mosteiro, A., Fernandes, P. G., Armstrong, F., and Greenstreet, S. P. R. 2004. A dual frequency algorithm for the identification of sandeel school echotraces. ICES Document CM, 12: 1–13.

Mulligan, T. 2000. Shallow water fisheries sonar: a personal view. Aquatic Living Resources, 13: 269–273.

Nucci, M., Costa, C., Scardi, M., and Cataudella, S. 2010. Preliminary observations on bluefin tuna (Thunnus thynnus, Linnaeus 1758) behaviour in captivity. Journal of Applied Ichthyology, 26: 95–98. Wiley Online Library.

Ona, E. and Barange, M. 1999. Single target recognition. CRR, Methodology for Target Strength Measurement. http://www.ices.dk/sites/pub/Publication%20Reports/Cooperative%20Research%20Report%20(CRR)/crr235/CRR235.pdf (Accessed 28 February 2017).

Pedersen, G., Korneliussen, R. J., and Ona, E. 2004. The relative frequency response, as derived from individually separated targets on cod, saithe and Norway pout. ICES. http://brage.bibsys.no/xmlui/handle/11250/100629 (Accessed 25 February 2016).

Pérez-Arjona, I., Godinho, L. M. C., and Espinosa, V. 2018. Numerical Simulation of Target Strength Measurements from Near to Far Field of Fish Using the Method of Fundamental Solutions. Acta Acustica united with Acustica, 104: 25–38.

Puig-Pons, V., Muñoz-Benavent, P., Pérez-Arjona, I., Ladino, A., Llorens-Escrich, S., Andreu-García, G., Valiente-González, J. M., *et al.* 2022. Estimation of Bluefin Tuna (Thunnus thynnus) mean length in sea cages by acoustical means. Applied Acoustics, 197: 108960.

Rodríguez-Sánchez, V., Encina-Encina, L., Rodríguez-Ruiz, A., and Sánchez-Carmona, R. 2016. Do close range measurements affect the target strength (TS) of fish in horizontal beaming hydroacoustics? Fisheries Research, 173: 4–10.

Schaefer, K. M. 1999. Comparative study of some morphological features of yellowfin (Thunnus albacares) and bigeye (Thunnus obesus) tunas. Inter-American Tropical Tuna Commission.

Simmonds, E. J., and MacLennan, D. N. 2005. Fisheries acoustics: theory and practice. Fish and aquatic resources series. Blackwell Science, Oxford ; Ames, Iowa. 437 pp.

Sobradillo, B., Boyra, G., Martinez, U., Carrera, P., Peña, M., and Irigoien, X. 2019. Target Strength and swimbladder morphology of Mueller's pearlside (Maurolicus muelleri). Scientific Reports, 9: 1–14.

Soule, M., Hampton, I., and Barange, M. 1996. Potential improvements to current methods of recognizing single targets with a split-beam echo-sounder. ICES Journal of Marine Science: Journal du Conseil, 53: 237–243.

Zhang, J., Chen, Z., Chen, G., Zhang, P., Qiu, Y., and Yao, Z. 2015. Hydroacoustic studies on the commercially important squid Sthenoteuthis oualaniensis in the South China Sea. Fisheries research, 169: 45–51. Elsevier.

Zhang, J., Zhang, K., Chen, Z., Dong, J., and Qiu, Y. 2021. Hydroacoustic studies on Katsuwonus pelamis and juvenile Thunnus albacares associated with light fish-aggregating devices in the South China Sea. Fisheries Research, 233: 105765.

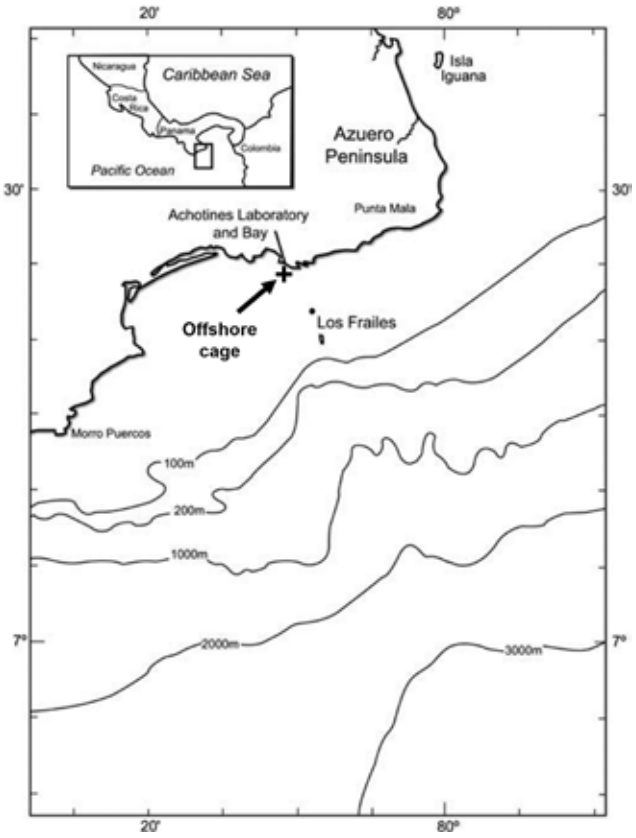

FIGURE 1. Location of the offshore cage outside Achotines Bay.

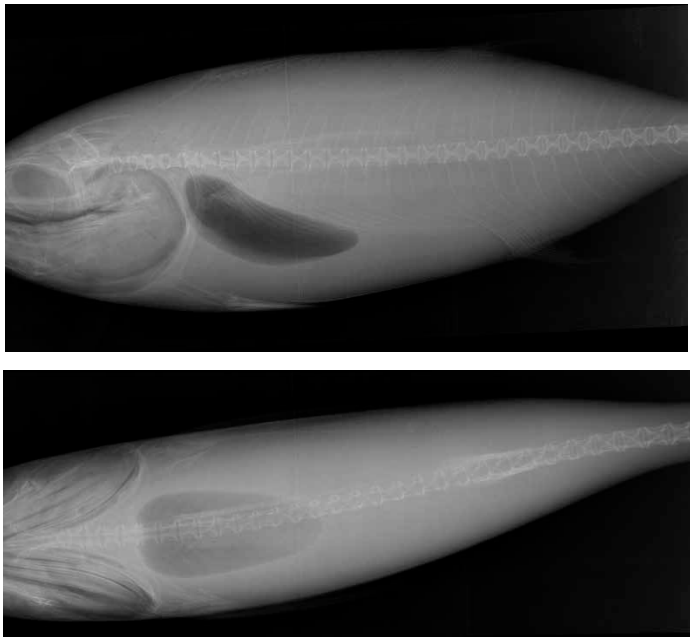

FIGURE 2. Example radiograph of one of the tuna in the cage, showing the morphology of the swim bladder in lateral (a) and ventral (b) views.

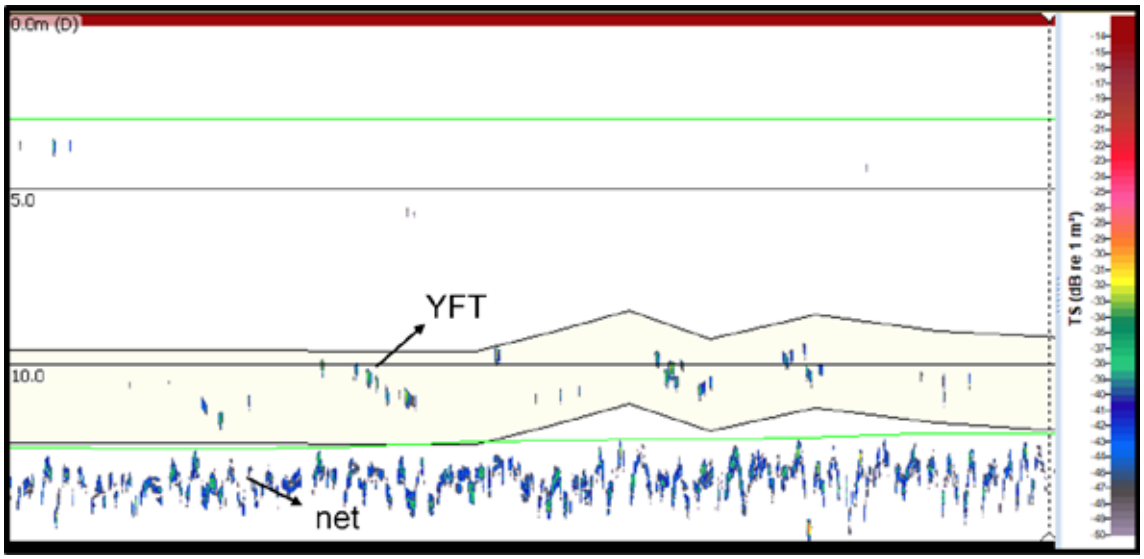

FIGURE 3. 38 kHz echogram showing the yellowfin tuna echoes close to the bottom of the cage.

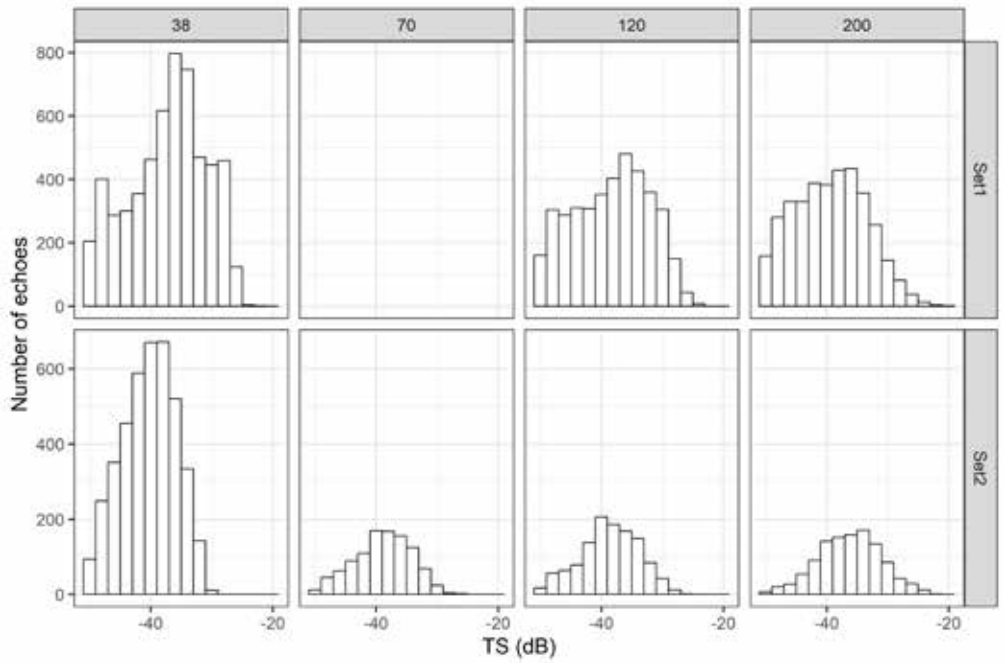

FIGURE 4. TS distributions obtained from single targets of the two sets of measurements at the four operational frequencies (kHz).

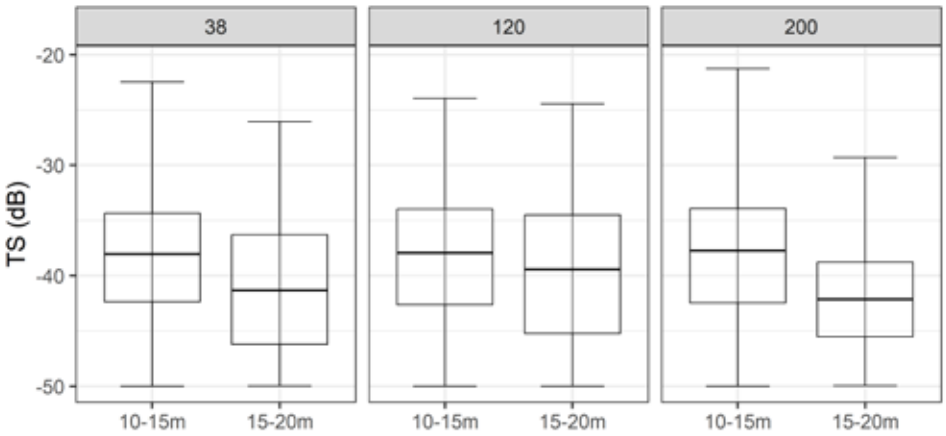

FIGURE 5. Boxplots illustrating the median, 1st and 3rd quartiles of the TS distributions at the three operational frequencies (kHz) common to both sets, at two depth layers. Error bars show the standard error of the mean.

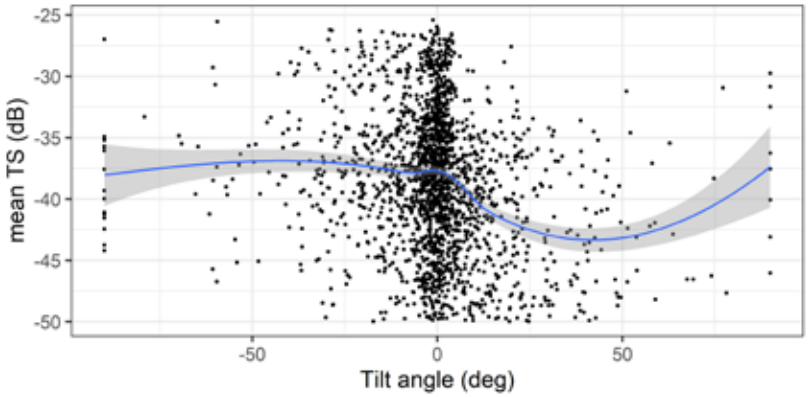

FIGURE 6. Mean TS variation against tilt angle at the four operational frequencies obtained from set 1, at 38 kHz. Tracks were filtered to -50 dB and a loess smoothing was applied.

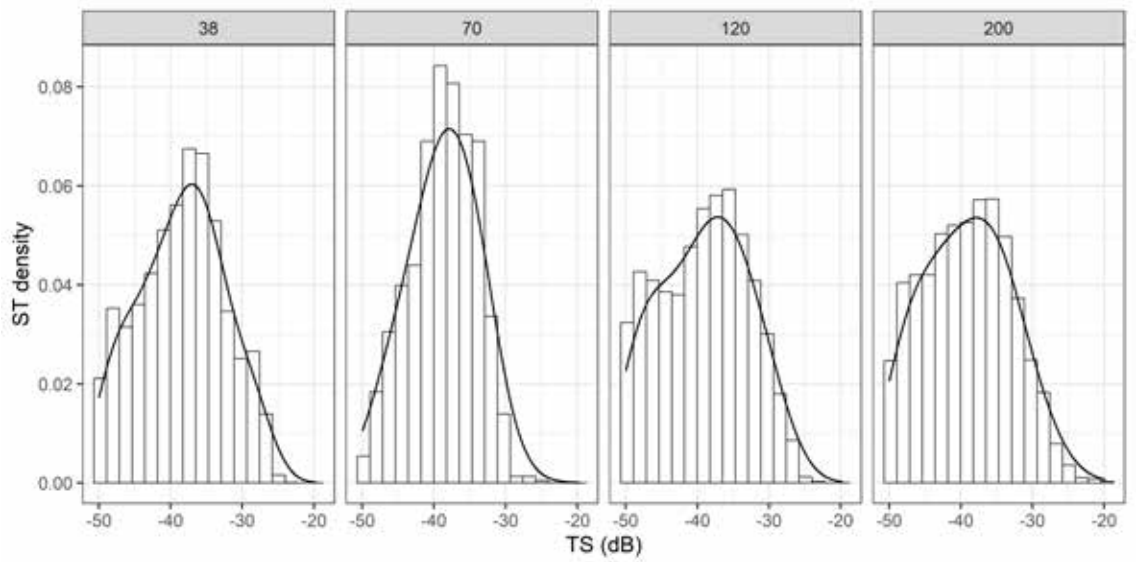

FIGURE 7. TS distribution with density curves obtained from single targets of live tuna sets (1a and 1b), filtered at -50 dB at the four operational frequencies (kHz).

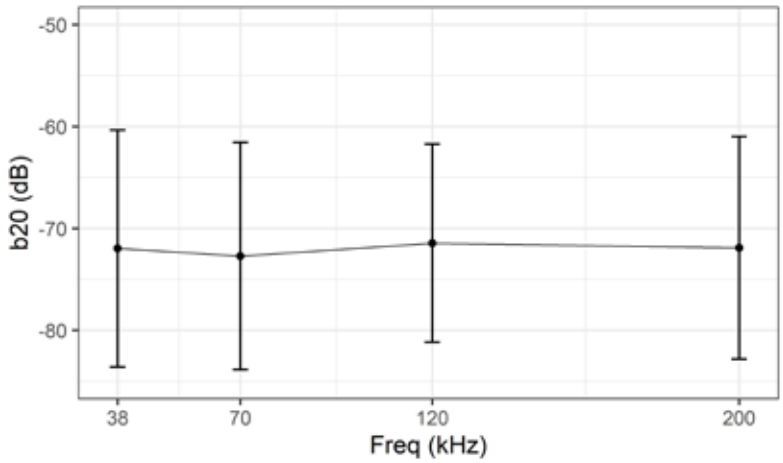

FIGURE 8. Frequency response of the mode of b_{20} values obtained from yellowfin tuna single target detections at the four frequencies of study.

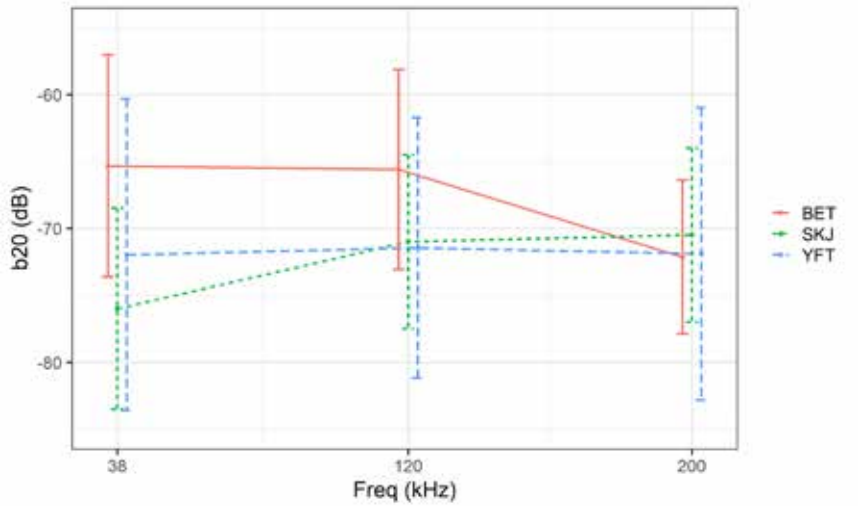

FIGURE 9. Frequency response of the b_{20} values from BET, YFT and SKJ. Error bars illustrate the standard deviation.

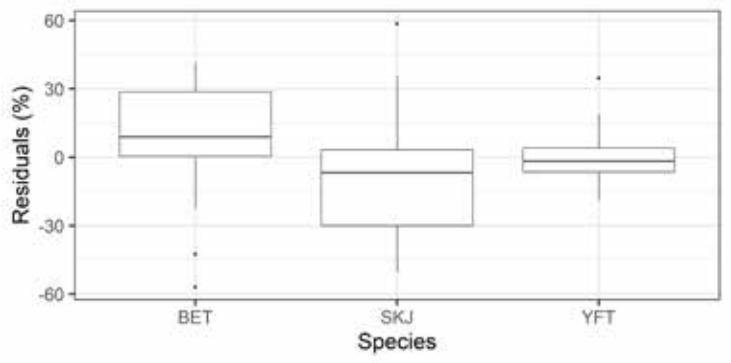

FIGURE 10. Residuals of the discrimination algorithm per species.

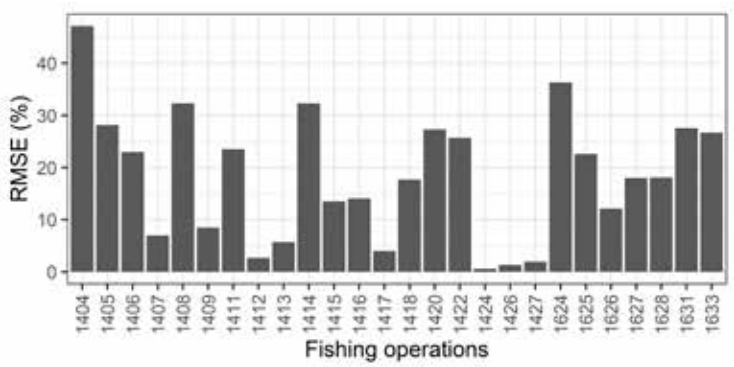

FIGURE 11. Error (RMSE) of the mask performance by fishing operations.

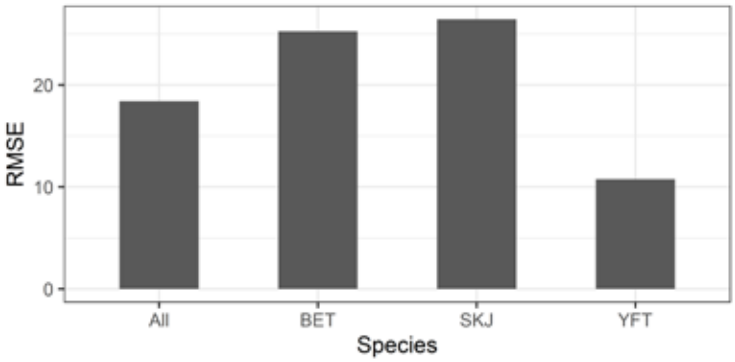

FIGURE 12. Error (RMSE) of the mask performance calculated by species and overall error.

TABLE 1. Biological measurements from fish body (TL: total length, FL: fork length, width, height and weight), and swimbladder. Z is the depth at which the diameter of the acoustic beam cross-section equals the fish or swimbladder length. Specimen marked with (*) is dead and used for controlled range experiment.

		Fish						Swimbladder			
Year	**Set**	**TL**	**FL**	**Z**	**Width**	**Height**	**Weight**	**Length**	**Z**	**Width**	**Area**
		cm	cm	m	cm	cm	kg	cm	m	cm	cm^2
2016	1	57	51.9	4.7	9.5	13	2.9	11.4	0.9	3.1	28.0
2016	1	70.8	64.4	5.8	11	15	3.9	12.2	1.0	4.1	38.8
2016	1	45.2	41.1	3.7	7.5	10.5	1.52	9.3	0.8	2.7	19.8
2016	1	59	53.7	4.8	10	13.5	3.16	12.5	1.0	3.8	37.6
2022	2	58	54.4	4.7	9.3	13.4	5.8	13.0	1.1	3.2	32.7
2022	2	56.2	51.4	4.6	8.5	13.2	5.25	10.7	0.9	3.4	28.6

TABLE 2. Calibrated echosounder settings used for measurements.

Year	Units	2016			2022			
Frequency	kHz	38	120	200	38	70	120	200
Pulse duration	µs	512	512	512	512	512	512	512
Power	W	2000	250	150	2000	750	250	150
Gain	dB	26.62	27	26.2	26.76	27	25.8	25.5
Sa correction	dB	-1.19	-0.41	-0.39	-0.59	-0.26	-0.11	-0.22
Sphere TS	dB	-42.04	-39.83	-39.45	-42.04	-40.56	-39.83	39.45

Table 3. Parameters used in the single target detection (SED) and tracking algorithms.

SED algorithm			Tracking algorithm		
Pulse length determination level	dB	6	Min. number of single targets in a track		3
Min/max normalized pulse length		0.7/1.5	Max number of pings in a track	pings	3
Maximum beam compensation	dB	15	Maximum gap between single targets	pings	5
Maximum standard deviation of axis angles	degrees	0.6	Exclusion distance (major axis/minor axis/range)	m	4/4/0.1